Adaptive Feedback Linearizing Control of a Gas Liquid Cylindrical Cyclone

Sveinung Johan Ohrem[1†], Torstein Thode Kristoffersen[1], Christian Holden[1]

1) Department of Mechanical and Industrial Engineering, Faculty of Engineering,
NTNU Norwegian University of Science and Technology, Trondheim, Norway, †: Corresponding author, sveinung.j.ohrem@ntnu.no

***Abstract*—As subsea production of oil and gas reaches deeper and more remote waters, the need for more compact separation equipment arises. The gas liquid cylindrical cyclone (GLCC) is a widely used separation device in topside facilities, but has yet to reach the same popularity subsea. The GLCC separates gas and liquid by inducing a swirl on the multiphase flow. Because of its small size, the GLCC is sensitive to flow variations which may reduce separation performance. The performance of the GLCC can be improved by control. In this paper we consider a nonlinear dynamic model of a GLCC containing unmeasured variables and states. We present an adaptive feedback linearizing controller and prove that the origin of the gas pressure and liquid level error systems are locally asymptotically stable in the sense of Lyapunov on a specified domain. The model and controller are implemented in Simulink and simulations show that the controller works very well, even with uncertainties in assumed known parameters, and measurement noise.**

I. Introduction

The gas liquid cylindrical cyclone or GLCC is a widely used separation device and is currently installed in over 6000 onshore gas production and processing plants around the world [1]. While popular in onshore production, the GLCC has yet to reach the same popularity in subsea and offshore production and processing facilities.

Subsea separation and gas-liquid separation in particular is described by [2] as an enabler for (i) more efficient liquid boosting, (ii) longer range gas compression from subsea to onshore, (iii) cost efficient hydrate management, (iv) more efficient riser slug depression and (v) access to challenging field developments. Subsea separation is also considered one of the main enablers for what is referred to as *Subsea Factory*, an all subsea oil and gas production facility concept able to produce and deliver oil and gas directly to customers without sending the produced fluids topside for processing [3].

The offshore oil and gas industry is currently relying on large vessels for separation. These vessels, commonly referred to as gravity separators, are robust and have high performance, but their use are limited by their size. In ultra deep waters ($\geq$ 3000 m), the required size of the gravity separators makes the installation and maintenance economically challenging [2]. When the size of gravity separators increases, so does their weight and there is a limited amount of ships available for installation of such large vessels [1]. This is why the offshore and subsea industry is leaning towards more compact separation technology such as the GLCC.

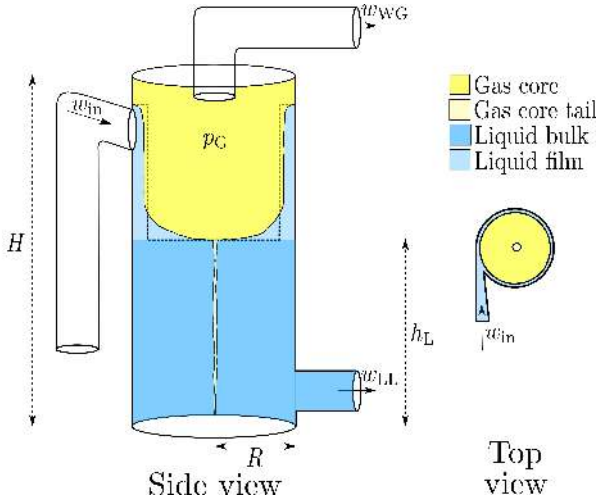

Fig. 1. Schematic of a GLCC.

The GLCC is equipped with a downward inclined tangential inlet and two outlets. It separates gas and liquid by inducing a swirl on the multiphase flow. The difference in density between the phases and the centrifugal forces induced by the swirl will cause the liquid to migrate to the walls and the gas to the center. The migration of the liquid creates a falling and swirling liquid film along the walls and the liquid accumulates at the bottom of the GLCC, establishing a liquid level. The swirling gas creates a gas core that penetrates the liquid level. A schematic of a typical GLCC is shown in Fig. 1.

The GLCC has many applications, e.g, multiphase metering, slug dampening and bulk separation [4]. When used as a bulk separator, the operational objective is to keep the gas and liquid quality within some specified requirements as well as minimizing downstream flow variations. Because of its small volume, the GLCC is sensitive to inlet flow variations. These variations are always present and may cause a significant reduction in separation performance. This directly affects downstream equipment like pumps and compressors and may cause economic loss.

The performance of the GLCC can be improved by control. In [5], a dynamic model of the GLCC is derived and PI and PD controllers are used to stabilize the pressure and liquid

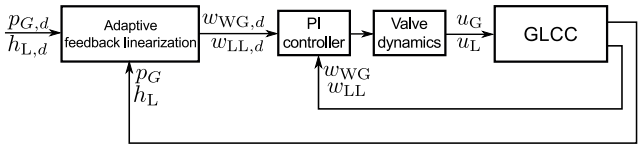

Fig. 2. Cascade control structure. The adaptive feedback linearizing controller calculates desired flows of liquid and gas and the PI controller adjusts the valves so the correct flows are reached.

level, respectively. The model used does not account for imperfect separation. In [6] a control strategy that provides unique valve positions for given flow conditions is presented. This strategy is similar to a gain-scheduling strategy and is able to stabilize the liquid level with different inflow conditions. In [7], a feed forward control scheme is combined with traditional feedback control to counteract the effect variations in the inlet flow has on the liquid level. Results show a significant decrease in level fluctuations when using the feed forward controller. An adaptive control method is presented in [8] where an adaptive tuning algorithm run on a microcontroller is used to reduce the movement of the liquid control valve while maintaining the desired liquid level.

A common factor in [5]–[8] is that the model used only considers the liquid level and gas pressure and does not take the separation dynamics into account; they assume perfect separation.

More recently, a control-oriented model of a GLCC including the phenomena of liquid carry over (LCO) and gas carry under (GCU) has been developed [9]. This model used empirical data for GCU and LCO calculations and thus gave a more correct representation of the dynamics of a GLCC. A feed forward control strategy was implemented and it was shown that the GCU or LCO can be limited, but the control strategy induced oscillations in the control valve and outlet flows that may damage the valve and cause problems for downstream process equipment like compressors and pumps.

In this paper we consider the model derived in [10]. This model is based on the physical mechanisms of GCU and LCO, includes more dynamics and hence enables model-based controller design. The model has been used to derive a feedback linearizing controller [11] and in this paper we relax some of the assumptions and requirements of [11] and derive an adaptive feedback linearizing controller. Local asymptotic stability, in the sense of Lyapunov, of the liquid level and gas pressure is proven and the results are verified in simulations. These also show that the controller is robust to parameter uncertainty and measurement noise. Our proposed controller provides us with desired outflow of liquid and gas which are used in a cascade control structure. The desired outlet flows are sent to a PI controller that operates the outlet valves for gas and liquid. See Fig. 2.

The paper is divided into the following sections: Section II describes the model. The proposed controller is derived in Section III. Section IV presents the results and Section V concludes the paper.

II. Dynamic model

The dynamic model of the GLCC separator used to study control was presented in [10] with only immediate separation of the inlet flow. The model was later extended to also describe continuous separation [12]. The following section provides a brief summary of this model.

The model consists of four mass balances and includes separation performance. The separation performance is described by four nonlinear separation factors; two describing immediate separation of the inlet gas-liquid flow and two describing the continuous separation between the gas and liquid volumes inside the GLCC separator.

The incomplete separation of the gas-liquid inlet flow results in a gas volume containing liquid droplets and a liquid volume containing gas bubbles. Therefore, the gas volume is called wet gas (WG) and the liquid volume is called light liquid (LL).

The dynamic model is on state-space form with the following states:

- $m_{\mathrm{LL,L}}$: accumulated liquid in LL [kg]
- $m_{\mathrm{LL,G}}$: accumulated gas in LL [kg]
- $m_{\mathrm{WG,L}}$: accumulated liquid in WG [kg]
- $m_{\mathrm{WG,G}}$: accumulated gas in WG [kg] .

The ordinary differential equations describing the dynamics are given by

$$\dot{m}_{\mathrm{LL,L}} = w_{\mathrm{in,L}} - w_{\mathrm{im,L}} + w_{\mathrm{L2LL}} - w_{\mathrm{LL,L}} \tag{1}$$

$$\dot{m}_{\mathrm{LL,G}} = w_{\mathrm{im,G}} - w_{\mathrm{G2WG}} - w_{\mathrm{LL,G}} \tag{2}$$

$$\dot{m}_{\mathrm{WG,L}} = w_{\mathrm{im,L}} - w_{\mathrm{L2LL}} - w_{\mathrm{WG,L}} \tag{3}$$

$$\dot{m}_{\mathrm{WG,G}} = w_{\mathrm{in,G}} - w_{\mathrm{im,G}} + w_{\mathrm{G2WG}} - w_{\mathrm{WG,G}}, \tag{4}$$

where $\dot{m}_{\mathrm{LL,L}}$ and $\dot{m}_{\mathrm{LL,G}}$ are the time derivatives of liquid and gas in the LL, respectively, $\dot{m}_{\mathrm{WG,L}}$ and $\dot{m}_{\mathrm{WG,G}}$ are the time derivatives of liquid and gas in the WG, respectively, $w_{\mathrm{in,L}}$ and $w_{\mathrm{in,G}}$ are the inlet mass flows of liquid and gas, respectively, $w_{\mathrm{LL,L}}$ and $w_{\mathrm{LL,G}}$ are the outlet mass flows of liquid and gas from the LL, respectively, $w_{\mathrm{WG,L}}$ and $w_{\mathrm{WG,G}}$ are the outlet mass flow of liquid and gas from the WG, respectively.

The immediate separation (the mass flows $w_{\mathrm{im,L}}$ and $w_{\mathrm{im,G}}$) describe the separation of the inlet liquid to the WG and inlet gas to the LL, respectively, while the continuous separation is described by the mass flows w_{L2LL} and w_{G2WG} describing the continuous separation of liquid from the WG to the LL and of gas from the LL to the WG, respectively.

Gas mass fractions are generally defined as

$$\beta_{\mathrm{x}} = \frac{m_{\mathrm{x,G}}}{m_{\mathrm{x,L}} + m_{\mathrm{x,G}}}, \tag{5}$$

where $\beta_{\mathrm{x}} \in [0, 1]$ is the gas mass fraction of x where x can represent either inlet, LL or WG.

The definition (5) is used to divide the multiphase flows into separate gas and liquid flows yielding

$$w_{\mathrm{x}} = w_{\mathrm{x,L}} + w_{\mathrm{x,G}} = (1 - \beta_{\mathrm{x}}) w_{\mathrm{x}} + \beta_{\mathrm{x}} w_{\mathrm{x}}. \tag{6}$$

The separation performance is determined by the amount of LCO and GCU that occurs at any given time. These phenomena are described by nonlinear separation factors resulting in highly nonlinear dynamics. The separation flows are described as

$$w_{\text{im,y}} = \epsilon_{\text{im,y}} w_{\text{in,y}} \tag{7}$$

$$w_{\text{y2z}} = \epsilon_{\text{y}} \beta_{\text{z}} m_{\text{z,y}} \tag{8}$$

where $\epsilon_{\text{im,y}} \in [0,1]$ is the immediate separation factor of y from the inlet flow and $\epsilon_{\text{y}} \in [0,1]$ is the continuous separation factor of y to z. The subscript y represents either gas or liquid, while z represents either LL or WG. The separation factors are highly nonlinear functions of the states and not further described this section. The interested reader is referred to [10] and [12] for details.

The liquid level h_L and gas pressures p_G are given by

$$h_{\text{L}} = \frac{m_{\text{LL,L}} + m_{\text{LL,G}}}{a} \tag{9}$$

$$p_{\text{G}} = \frac{b m_{\text{WG,G}}}{aH - (m_{\text{LL,L}} + m_{\text{LL,G}})} \ , \tag{10}$$

where H is the total tank height and $a = \rho_L A > 0$ and $b = \frac{\rho_L RT}{M_{\text{WG,G}}} > 0$ are model parameters. We assume that the liquid level and gas pressure are available as measurements and thus, these variables constitute the controlled variables.

III. Control

A. State transformation

The following state transformation was first presented in [11], but is repeated here for completeness. The dynamics of the liquid phase is governed by the liquid and hence is described by the state x_1. Since the weight of the liquid is much higher than the weight of the gas, the gas dynamics are considered as a coupling of the liquid and gas dynamics and hence it is separated into two states, x_2 and x_3. The new states are

$$x \triangleq \begin{bmatrix} x_1 \\ x_2 \\ x_3 \end{bmatrix} = \begin{bmatrix} m_{\text{LL,L}} + m_{\text{LL,G}} \\ m_{\text{WG,L}} \\ m_{\text{WG,G}} \end{bmatrix} \tag{11}$$

Differentiating (11) with respect to time gives

$$\dot{x}_1 = \dot{m}_{\text{LL,L}} + \dot{m}_{\text{LL,G}} = f_1(\cdot) + f_{1,s}(\cdot) - w_{\text{LL}} \tag{12}$$

$$\dot{x}_2 = \dot{m}_{\text{WG,L}} = f_{2,s}(\cdot) - w_{\text{WG,L}} \tag{13}$$

$$\dot{x}_3 = \dot{m}_{\text{WG,G}} = f_3(\cdot) + f_{3,s}(\cdot) - w_{\text{WG,G}} \tag{14}$$

where

$$f_1(\cdot) = w_{\text{in,L}} \tag{15}$$

$$f_{1,s}(\cdot) = -w_{\text{im,L}} + w_{\text{L2LL}} + w_{\text{im,G}} - w_{\text{G2WG}} \tag{16}$$

$$f_{2,s}(\cdot) = w_{\text{im,L}} - w_{\text{L2LL}} \tag{17}$$

$$f_3(\cdot) = w_{\text{in,G}} \tag{18}$$

$$f_{3,s}(\cdot) = -w_{\text{im,G}} + w_{\text{G2WG}} \tag{19}$$

where $w_{\text{LL}} = w_{\text{LL,L}} + w_{\text{LL,G}}$. Function arguments will be left out for the rest of this paper. The inlet mass flow is described by f_1 and f_3 and the immediate and continuous separation is described by $f_{1,s}$, $f_{2,s}$,$f_{3,s}$. We assume these functions to be slowly time-varying. We assume that the system is designed such that $||w_{\text{LL}}||_\infty > ||f_1 + f_{1,s}||_\infty$ and $||w_{\text{WG,G}}||_\infty > ||f_3 + f_{3,s}||_\infty$, i.e., the possible outflow is always higher than the highest possible inflow and separation flow (this allows draining the tank no matter the inflow). The inlet functions f_1 and f_3 are assumed to satisfy the following conditions

$$0 < \delta_1 \leq f_1 \leq \delta_2 w_{\text{LL,max}} \tag{20}$$

$$0 < \delta_3 \leq f_3 \leq \delta_4 w_{\text{WG,max}} \tag{21}$$

with $\delta_1, \delta_3 > 0$, $\delta_2, \delta_4 \in (0,1)$ and $w_{\text{LL,max}}$ and $w_{\text{WG,max}}$ are the maximum possible outlet mass flows of liquid and gas respectively, giving well defined minima and maxima of the functions f_1 and f_3. Furthermore, $w_{\text{LL}} \in [0, w_{\text{LL,max}}]$ and $w_{\text{WG,L}} + w_{\text{WG,G}} = w_{\text{WG}} \in [0, w_{\text{WG,max}}]$.

We want to control the liquid level and the gas pressure. In the transformed state-space, these variables are given by

$$y_1 = h_L = \frac{1}{a} x_1 \tag{22}$$

$$y_2 = p_G = \frac{b}{aH - x_1} x_3 \ . \tag{23}$$

The physical domain of the system is defined by the operational limits for liquid level and gas pressure, namely h_{HAL}, h_{LAL}, p_{HAL} and p_{LAL} where HAL refers to the high alarm limit and LAL to the low alarm limit. Reaching any of these limits would initiate system shut down. Thus the operating domain is defined as

$$\mathcal{O}_1 = \left\{ y \in \mathbb{R}^2 \middle| h_{\text{HAL}} > y_1 > h_{\text{LAL}}, p_{\text{HAL}} > y_2 > p_{\text{LAL}} \right\}. \tag{24}$$

Differentiating the outputs y_1 and y_2 gives

$$\dot{y}_1 = \frac{1}{a} \left[f_1 + f_{1,s} - w_{\text{LL}} \right] \tag{25}$$

$$\dot{y}_2 = \frac{b}{aH - x_1} \left[f_3 + f_{3,s} - \frac{x_3}{x_2 + x_3} w_{\text{WG}} + \frac{x_3 (f_1 + f_{1,s} - w_{\text{LL}})}{aH - x_1} \right] \ . \tag{26}$$

The input appears in the first derivative of both outputs, hence each output has a relative degree of 1, summing up to a total relative degree of 2. Since the system has 3 states the transformed system has 1 internal state and 2 external states. The state transformation is given by

$$z = T(x) = [\eta, \xi_1, \xi_2]^T \tag{27}$$

where $\xi = y = [y_1, y_2]^T$ is the external state and $\eta = \phi(x)$ is the internal state. It is shown in [11] that by choosing the internal state as $\eta = \frac{x_2}{x_3}$ and extending the physical domain $\mathcal{O}_1$ to

$$\mathcal{O}_2 = \left\{ z \in \mathbb{R}^3 \middle| \eta > 0, h_{\text{HAL}} > \xi_1 > h_{\text{LAL}}, p_{\text{HAL}} > \xi_2 > p_{\text{LAL}} \right\} \tag{28}$$

we can apply the state transformation

$$T(x) = \left[\frac{x_2}{x_3}, \frac{x_1}{a}, \frac{b x_3}{aH - x_1} \right]^T \tag{29}$$

which is a diffeomorphism on

$$\mathcal{I} = \Big\{ x \in \mathbb{R}^3 \big| x_1 > 0, ah_{\text{HAL}} > x_2 > ah_{\text{LAL}}, \frac{aHp_{\text{HAL}}}{b} > x_3 > \frac{aHp_{\text{LAL}}}{b} \Big\} \quad (30)$$

because both $T(x)$ and $T^{-1}(x)$ exist and are continuously differentiable on the domain. The resulting transformed system is given as

$$\dot{\eta} = \frac{b}{a\xi_2(H-\xi_1)} \left[f_{2,s} - \eta(f_3 + f_{3,s}) \right] \quad (31)$$

$$\dot{\xi}_1 = \frac{1}{a} \left[f_1 + f_{1,s} - w_{\text{LL}} \right] \quad (32)$$

$$\dot{\xi}_2 = \mathcal{F} \left[f_3 + f_{3,s} - \frac{1}{\eta+1} w_{\text{WG}} + \frac{\xi_2}{b} \left(f_1 + f_{1,s} - w_{\text{LL}} \right) \right] \quad (33)$$

where $\mathcal{F} = \frac{b}{a(H-\xi_1)}$.

B. Adaptive feedback linearizing controller

In the following we will assume that the system parameters a and b are known as well as the total tank height H.

We want the external states to track the constant references $\xi_{1,d}$ and $\xi_{2,d}$, which are the desired liquid level and gas pressure, respectively. We define the error variables $\tilde{\xi}_1 = \xi_1 - \xi_{1,d}$ and $\tilde{\xi}_2 = \xi_2 - \xi_{2,d}$.

To ensure local asymptotic stability when tracking a reference, the input to the system must be allowed to take negative values. This is impossible if we consider the outflows w_{LL} and w_{WG} as inputs, since $w_{\text{LL}}, w_{\text{WG}} \geq 0$. Instead, we consider the net flow $\Delta w_{\text{LL}} = w_{\text{LL}} - f_1$ as input to system (32) and the net flow $\Delta w_{\text{WG}} = w_{\text{WG}} - f_3$ as input to system (33). These inputs satisfy

$$\underline{w}_{\text{LL}} \leq \Delta w_{\text{LL}} \leq \overline{w}_{\text{LL}} \quad (34)$$

$$\underline{w}_{\text{WG}} \leq \Delta w_{\text{WG}} \leq \overline{w}_{\text{WG}} \quad (35)$$

where $\underline{w}_{\text{LL}} = -\delta_2 w_{\text{LL,max}} < 0$, $\underline{w}_{\text{WG}} = -\delta_4 w_{\text{WG,max}} < 0$, $\overline{w}_{\text{LL}} = w_{\text{LL,max}} - \delta_1 > 0$ and $\overline{w}_{\text{WG}} = w_{\text{WG,max}} - \delta_3 > 0$.

The error dynamics are given by

$$\dot{\eta} = \frac{b}{a(\tilde{\xi}_2 + \xi_{2,d})(H - \tilde{\xi}_1 - \xi_{1,d})} \left[f_{2,s} - \eta(f_3 + f_{3,s}) \right] \quad (36)$$

$$\dot{\tilde{\xi}}_1 = \frac{1}{a} \left[f_{1,s} - \Delta w_{\text{LL}} \right] \quad (37)$$

$$\dot{\tilde{\xi}}_2 = \mathcal{F} \left[f_{3,s} - \Delta w_{\text{WG}} + \sigma w_{\text{WG}} + \frac{\xi_2}{b} (f_{1,s} - \Delta w_{\text{LL}}) \right] \quad (38)$$

where $\sigma = 1 - \frac{1}{\eta+1}$.

The error systems (37) and (38) are written in linear parameterized form as

$$\dot{\tilde{\xi}}_1 = \phi_1 (\theta_1 - \Delta w_{\text{LL}}) \quad (39)$$

$$\dot{\tilde{\xi}}_2 = \theta_2^{\text{T}} \phi_2 - \mathcal{F}(\Delta w_{\text{WG}} + \frac{\xi_2}{b} \Delta w_{\text{LL}}) \quad (40)$$

where $\phi_1 = 1/a$, $\theta_1 = f_{1,s}$, $\theta_2 = \begin{bmatrix} f_{3,s} & \sigma & \theta_1 \end{bmatrix}^{\text{T}}$ and $\phi_2 = \begin{bmatrix} \mathcal{F} & \mathcal{F} w_{\text{WG}} & \frac{\mathcal{F}\xi_2}{b} \end{bmatrix}^{\text{T}}$. We assume that the unknowns, θ_1 and θ_2 are small ($|\theta_1| \ll |\overline{w}_{\text{LL}}|, ||\theta_2||_2 \ll |\overline{w}_{\text{WG}} + \overline{w}_{\text{LL}}|$) and constant or slowly varying with $\dot{\theta}_1 = \dot{\theta}_2 = 0$.

Theorem 1. *Choosing*

$$\Delta w_{LL} = \hat{\theta}_1 + \frac{1}{\phi_1} k_1 \tilde{\xi}_1 \quad (41)$$

$$\Delta w_{WG} = -\frac{\xi_2}{b} \hat{\theta}_1 - \frac{\xi_2}{b\phi_1} k_1 \tilde{\xi}_1 + \frac{1}{\mathcal{F}} \left(k_2 \tilde{\xi}_2 + \hat{\theta}_2^T \phi_2 \right) \quad (42)$$

where $k_1, k_2 > 0$, as input to (39) *and* (40)*, respectively and using*

$$\dot{\hat{\theta}}_1 = \gamma_1 \textit{Proj}(\hat{\theta}_1, \phi_1 \tilde{\xi}_1) \quad (43)$$

$$\dot{\hat{\theta}}_2 = \Gamma_2 \textit{Proj}(\hat{\theta}_2, \phi_2 \tilde{\xi}_2) \quad (44)$$

where $\gamma_1, \Gamma_2 > 0$, as update laws for the estimated parameters $\hat{\theta}_1$ and $\hat{\theta}_2$ renders the origin of the error systems (39) *and* (40) *locally asymptotically stable.*

Proof. Inserting (41) into (39) gives

$$\dot{\tilde{\xi}}_1 = -k_1 \tilde{\xi}_1 + \tilde{\theta}_1 \phi_1 \ , \quad (45)$$

where $\tilde{\theta}_1 = \theta_1 - \hat{\theta}_1$. Inserting (41) and (42) into (40) gives

$$\dot{\tilde{\xi}}_2 = -k_2 \tilde{\xi}_2 + \tilde{\theta}_2^{\text{T}} \phi_2 \quad (46)$$

where $\tilde{\theta}_2 = \theta_2 - \hat{\theta}_2$. Consider the positive definite Lyapunov function candidate

$$V = \frac{1}{2}\tilde{\xi}_1^2 + \frac{1}{2}\tilde{\xi}_2^2 + \frac{1}{2\gamma_1}\tilde{\theta}_1^2 + \frac{1}{2}\tilde{\theta}_2^{\text{T}} \Gamma_2^{-1} \tilde{\theta}_2 \quad (47)$$

where $\gamma_1 > 0$ and $\Gamma_2 = \Gamma_2^{\text{T}} > 0$ are adaptation gains. The time derivative of (47) along the trajectories of the system (45), (46) is given by

$$\begin{aligned} \dot{V} &= -k_1 \tilde{\xi}_1^2 - k_2 \tilde{\xi}_2^2 + \tilde{\theta}_1 \phi_1 \tilde{\xi}_1 + \tilde{\theta}_2^{\text{T}} \phi_2 \tilde{\xi}_2 \\ &\quad + \frac{1}{\gamma_1} \tilde{\theta}_1 \dot{\tilde{\theta}}_1 + \tilde{\theta}_2^{\text{T}} \Gamma_2^{-1} \dot{\tilde{\theta}}_2 \quad (48) \\ &= -k_1 \tilde{\xi}_1^2 - k_2 \tilde{\xi}_2^2 + \tilde{\theta}_1 \left(\phi_1 \tilde{\xi}_1 + \frac{1}{\gamma_1} \dot{\tilde{\theta}}_1 \right) \\ &\quad + \tilde{\theta}_2^{\text{T}} \left(\tilde{\xi}_2 \phi_2 + \Gamma_2^{-1} \dot{\tilde{\theta}}_2 \right) \ . \quad (49) \end{aligned}$$

The projection operator in (43) and (44) ensures that the estimates $\hat{\theta}_1$ and $\hat{\theta}_2$ are bounded and prevents windup issues due to the bounds on the control inputs Δw_{LL} and Δw_{WG}. The projection operator is defined in [13, App. B] as

$$\text{Proj}(\hat{\theta}, y) \triangleq \begin{cases} y \ \text{if} \ g(\hat{\theta}) < 0 \vee g(\hat{\theta}) \geq 0 \wedge \nabla g^{\text{T}} y \leq 0 \\ y - \frac{\nabla g \nabla g^{\text{T}} y g(\hat{\theta})}{||\nabla g||^2}, \text{if} \ g(\hat{\theta}) \geq 0 \wedge \nabla g^{\text{T}} y > 0 \end{cases} \quad (50)$$

where the logic symbols $\vee$ and $\wedge$ represents *or* and *and*, respectively, and $g(\hat{\theta})$ is a smooth function

$$g(\hat{\theta}) = \frac{(\epsilon_\theta + 1)\hat{\theta}^{\text{T}}\hat{\theta} - \theta_{\text{max}}^2}{\epsilon_\theta \theta_{\text{max}}^2} \quad (51)$$

with $\epsilon_\theta > 0$ as the projection tolerance bound, $||\theta||_2^2 \leq \theta_{\max}^2$ and gradient $\nabla g(\hat{\theta}) = 2\frac{\epsilon_\theta+1}{\epsilon_\theta \theta_{\max}^2}\hat{\theta}$.

We choose a set Ω_0 such that $\theta_1 \in \Omega_0 \subset \Omega_1$ and $\hat{\theta}_1 \in \Omega_1$ and a set Ω_2 such that $||\theta_2||_2 \in \Omega_2 \subset \Omega_3$ and $\hat{\theta}_2 \in \Omega_3$.

Inserting the update laws (43) and (44) into (49) and utilizing the fact that $\dot{\theta}_1 = \dot{\theta}_2 = 0$, $\dot{\tilde{\theta}}_1 = \dot{\theta}_1 - \dot{\hat{\theta}}_1 = -\dot{\hat{\theta}}_1$ and $\dot{\tilde{\theta}}_2 = \dot{\theta}_2 - \dot{\hat{\theta}}_2 = -\dot{\hat{\theta}}_2$, gives

$$\begin{aligned}\dot{V} &= -k_1\tilde{\xi}_1^2 - k_2\tilde{\xi}_2^2 + \tilde{\theta}_1(\phi_1\tilde{\xi}_1 - \text{Proj}(\hat{\theta}_1, \phi_1\tilde{\xi}_1)) \qquad (52)\\ &\quad + \tilde{\theta}_2(\phi_2\tilde{\xi}_2 - \text{Proj}(\hat{\theta}_2, \phi_2\tilde{\xi}_2))\\ &\leq -k_1\tilde{\xi}_1^2 - k_2\tilde{\xi}_2^2 \ \leq 0 \ \forall \ \tilde{\xi}_1, \tilde{\xi}_2 \ . \qquad (53)\end{aligned}$$

where [13, Property B.2] ensures that $\tilde{\theta}_1(\phi_1\tilde{\xi}_1 - \text{Proj}(\hat{\theta}_1, \phi_1\tilde{\xi}_1)) \leq 0$ and $\tilde{\theta}_2(\phi_2\tilde{\xi}_2 - \text{Proj}(\hat{\theta}_2, \phi_2\tilde{\xi}_2)) \leq 0$.

This implies that $V(t) \leq V(0)$ and that the origin of the systems (45), (46), (43), (44) are stable [14, Th. 4.1]. We assume that the initial errors $\tilde{\xi}_1(t_0)$, $\tilde{\xi}_2(t_0)$ are bounded, and hence $\tilde{\xi}_1(t)$ and $\tilde{\xi}_2(t)$ are bounded.

The time derivative of $\dot{V}$ is

$$\ddot{V} = -2k_1\tilde{\xi}_1\dot{\tilde{\xi}}_1 - 2k_2\tilde{\xi}_2\dot{\tilde{\xi}}_2 \qquad (54)$$

where all signals are bounded and consequently $\ddot{V}$ is bounded and $\dot{V}$ is uniformly continuous. By application of Barbălat's lemma in the same manner as in [15], convergence of $\dot{V}$ to zero and consequently asymptotic convergence of $\tilde{\xi}_1$, $\tilde{\xi}_2$ to zero is guaranteed. From (43), (44), this in turn implies that $\dot{\hat{\theta}}_1$ and $\dot{\hat{\theta}}_2$ converge to zero asymptotically. Combining the proof of convergence with the proof of stability, we have proof of asymptotic stability in the sense of Lyapunov of the origins of the systems (39) and (40). □

In the error system (45), we are in fact guaranteed convergence of $\tilde{\theta}_1 \to 0$. We have shown that $\tilde{\xi}_1 \to 0 \implies \dot{\tilde{\xi}}_1 \to 0$ which is only true if $\tilde{\theta} \to 0$. In the error system (46), it is required that ϕ_2 is a persistently exciting (PE) signal in order to guarantee parameter convergence [16, Ch. 4.2]. Having this signal be sufficiently PE, however, is not desired, as the manipulated variable in ϕ_2 is the gas flow w_{WG} and enforcing PE on this signal would cause significant wear and tear on the valve controlling the gas flow. Since the focus of the controller is stabilization, not parameter estimation, having the ϕ_2 signal be sufficiently PE is not considered necessary.

Parameter convergence is not guaranteed when the controller is implemented on the more accurate model described in Section II, since our assumptions are not necessarily satisfied and we include valve dynamics in the simulations which alters the total dynamics of the system.

By replacing θ_1 and θ_2 with estimates $\hat{\theta}_1$ and $\hat{\theta}_2$, we relax the assumptions from [11], where these are assumed known.

The internal state η enters system (33) and it is important that this state is upper bounded and not equal to -1. It is shown in [11] that $0 < |\eta| \leq h(|\eta(t_0)|, t - t_0) < \infty$ where h is a class $\mathcal{KL}$ function, if certain inlet conditions are satisfied. We use the same system and inlet conditions in this paper as described in [11] and hence, the conditions are satisfied. The interested reader is referred to [11] for the full proof of boundedness of η.

C. Cascade control

In the stability analysis in the previous section, we defined the inputs to the error systems as Δw_{LL} and Δw_{WG}. Since the actual inputs to the GLCC are the valve openings of the liquid and gas valves, we need to transform this signal to a corresponding valve opening. This is done by a cascade control structure, as shown in Fig. 2.

We define the desired outlet flows of liquid and gas as $w_{\text{LL},d} = \Delta w_{\text{LL}} + f_1$ and $w_{\text{WG},d} = \Delta w_{\text{WG}} + f_3$ for the liquid and gas outlet, respectively. These flows are used as references to a PI controller that determines the corresponding valve opening. The PI controllers takes the form

$$u_{\text{L}} = -k_{\text{L}}\left((w_{\text{LL}} - w_{\text{LL},d}) + \frac{1}{\tau_L}\int_0^t (w_{\text{LL}} - w_{\text{LL},d})\,\text{d}t\right) \qquad (55)$$

$$u_{\text{G}} = -k_{\text{G}}\left((w_{\text{WG}} - w_{\text{WG},d}) + \frac{1}{\tau_G}\int_0^t (w_{\text{WG}} - w_{\text{WG},d})\,\text{d}t\right) \qquad (56)$$

where w_{LL} and w_{WG} are the actual mass flows through the valves. The PI controller parameters $k_L > 0$, $\tau_L > 0$, $k_G > 0$ and $\tau_G > 0$ are the proportional gain and integral time for the liquid and gas flow controllers.

IV. Results

A. Simulations of the simplified system

We first simulate the system (36)–(38) in Simulink to verify that the controller works on the system for which it is designed. We do not consider the dynamics of the separation factors or the uncertainty of the system parameters, i.e., the separation mass flows $f_{1,s}, f_{2,s}$ and $f_{3,s}$ are constants and the system parameters a, b and H are known exactly. We use Δw_{LL} and Δw_{WG} as inputs without considering valves, but using the bounds. The controller parameters used in this simulation is listed in Table I. As can be seen in Fig. 3, the controller is able to bring the states to the desired references as expected. We also see that the unknown parameter θ_1 is estimated correctly, but the parameter vector θ_2 is not correct as this would require a PE signal in the update law (44).

B. Simulations of the full system

We also simulate the closed-loop system on the more accurate model described in Section II, with varying inlet flows which in turn induces changes in the separation flows. The simulations are run for 3600 seconds and we use the variable-step ode15s solver. We assume a constant backpressure of 48 bar and a constant temperature of $60°$C. We also introduce the cascade controller and send the generated valve signals through a low-pass filter $h(s) = \frac{1}{2s+1}$ to emulate the valve dynamics seen in Fig. 2.

The inlet liquid mass flow changes between nominal ($\sim$ 9.5 kg/s), high ($\sim$ 19 kg/s) and low ($\sim$ 4.8 kg/s). The same goes for the inlet gas mass flow. This also changes between nominal ($\sim$ 2.4 kg/s), low ($\sim$ 1 kg/s) and high

TABLE I
PARAMETERS USED IN SIMULATION 1

Parameter	Value	Description
γ_1	1	Adaptation gain
Γ_2	$5 \times 10^{-5}\mathbf{I}^{3\times3}$	Adaptation gain
k_1	25	Feedback gain level controller
k_2	5	Feedback gain pressure controller

TABLE II
PARAMETERS USED IN SIMULATIONS 2 AND 3

Parameter	Value	Description
γ_1	5	Adaptation gain
Γ_2	$20 \times 10^{-5}\mathbf{I}^{3\times3}$	Adaptation gain
k_1	250	Feedback gain level controller
k_2	10	Feedback gain pressure controller
k_L, k_G	10	Cascade controller P gain
τ_L, τ_G	100	Cascade controller time constant

($\sim$ 3.4 kg/s). This results in 3 different inlet conditions, namely nominal, low gas / high liquid and high gas / low liquid. The inlet conditions are shown at the bottom of Fig. 4. We also introduce changes in the desired liquid level and gas pressure.

As bound on θ_1 we choose $\theta_{1,\max} = \overline{w}_{\text{LL}} = 22$ [kg/s] and for θ_2 we choose $||\theta_{2,\max}||_2 = \theta_{1,\max} + \overline{w}_{\text{WG}} = 27$ [kg/s]. The projection tolerance bound is chosen as $\epsilon_\theta = 1$ for both projection update laws.

As can be seen in Fig. 4, the controller performs very well. The states quickly converges to their desired values and the disturbances caused by the changes in inlet flows are attenuated. The desired outlet flows are tracked very well by the cascade controller. The controller parameters used in the simulation are listed in Table II.

To demonstrate the robustness of the controller we introduce an error to the variable ϕ_2, which is used in Δw_{WG} and in the update law for $\hat{\theta}_2$. More specifically, we multiply the values of a and b by 0.5 and 0.7, respectively. We also add white noise with a sample time of 1 second and a power of 0.0001 to all measurements. The results of this simulation are shown in Fig. 5. We see that even under these conditions, the controller performs well. The performance is of course limited by the dynamics of the valves and the fact that the noisy measurements are not filtered. We use the same controller parameters as in Simulation 2.

V. CONCLUSIONS

In this paper we have proposed an adaptive feedback linearizing controller for gas liquid cylindrical cyclones capable of asymptotically controlling the liquid level and gas pressure. The dynamics of the liquid level and gas pressure are affected by the nonlinear separation factors which cannot be measured. By applying a state transformation and using a Lyapunov approach we derived control laws for the liquid and gas outflows as well as update laws for the unknown parameters. We used a projection-based adaptation law preventing windup issues related to limitations of the control input.

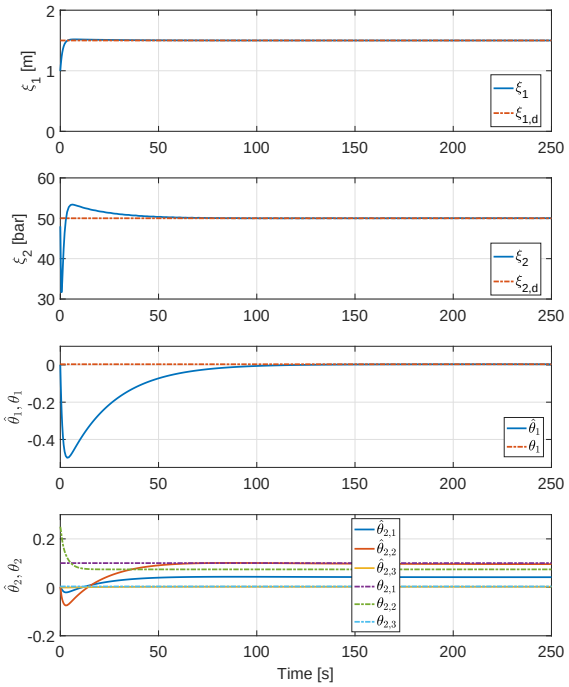

Fig. 3. The behaviour of the liquid level and gas pressure error systems with constant separation flows $f_{1,s}$, $f_{2,s}$ and $f_{3,s}$ and no valve dynamics.

The origins of the transformed system error dynamics were proven to be locally asymptotically stable in the sense of Lyapunov. We verified the theoretical results in three different simulations; one on the nominal system and two on a more complex model. In the first simulation scenario, the results match those expected from the theoretical results. In the two other simulation scenarios, in addition to using a more complex plant model, the calculated desired outflow was used in a cascade control setting with PI controllers as secondary controllers.

Simulations were carried out with and without measurement noise and parameter uncertainties. In both cases the controller is capable of tracking the desired references, indicating robustness of the controller. Parameter tracking, however, can not be guaranteed. The mathematical proof of boundedness of the error systems (39) and (40) under the presence of measurement noise is left as future work.

As future work we also recommend designing observers for the liquid level and gas pressure, as these measurements may not be available or they may be highly contaminated by noise and delays.

ACKNOWLEDGEMENTS

This work was carried out as a part of SUBPRO, a Research-based Innovation Centre within Subsea Production and Processing. The authors gratefully acknowledge the financial support from SUBPRO, which is financed by the Research Council of Norway, major industry partners, and NTNU.

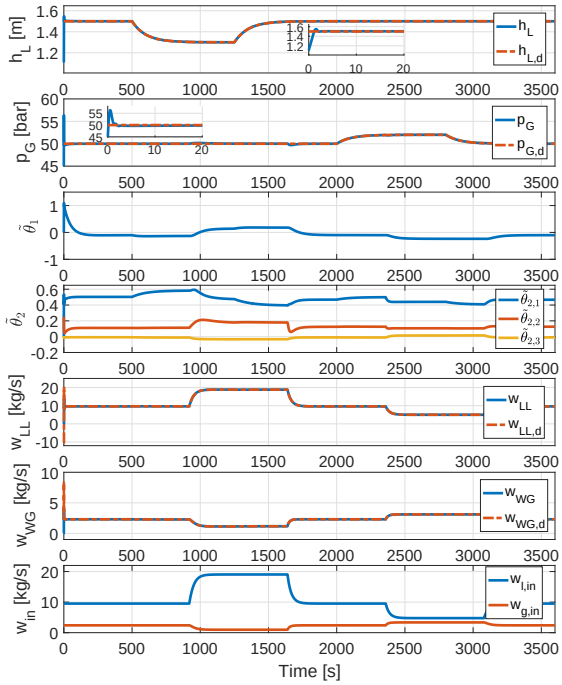

Fig. 4. Closed-loop behaviour with the full non-simplified dynamics.

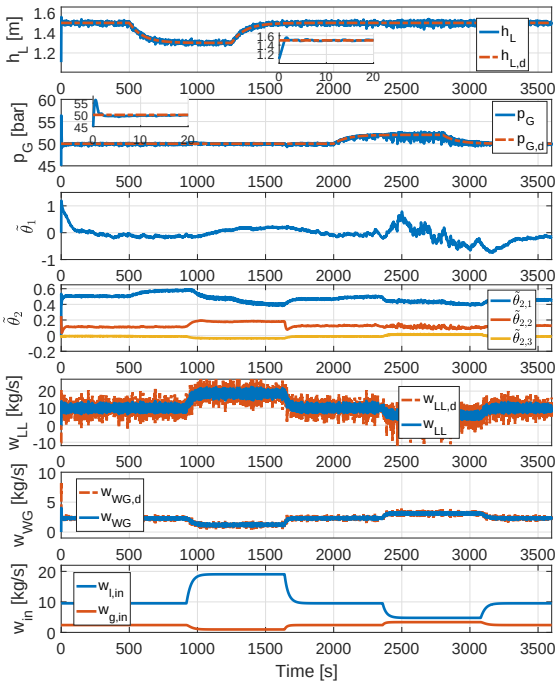

Fig. 5. Closed-loop behaviour with the full non-simplified dynamics with errors in the parameter ϕ_2 and measurement noise.

REFERENCES

[1] O. Kristiansen, Ø. Sørensen, and O. Nilssen, "CompactSep, compact subsea gas-liquid separator for high-pressure wellstream boosting," Offshore Technology Conference, 2016.

[2] A. Hannisdal, R. Westra, M. R. Akdim, A. Bymaster, E. Grave, and D. T. Teng, "Compact separation technologies and their applicability for subsea field development in deep water," in *Offshore Technology Conference*, Offshore Technology Conference, 2012.

[3] R. M. Ramberg, H. Rognoe, and O. Oekland, "Steps to the subsea factory," in *OTC Brasil*, Offshore Technology Conference, 2013.

[4] G. E. Kouba, S. Wang, L. E. Gomez, R. S. Mohan, and O. Shoham, "Review of the state-of-the-art gas-liquid cylindrical cyclone (glcc) technology-field applications," in *International Oil & Gas Conference and Exhibition in China*, Society of Petroleum Engineers, 2006.

[5] S. Wang, R. Mohan, O. Shoham, and G. Kouba, "Dynamic simulation and control system design for gas-liquid cylindrical cyclone separators," in *SPE Annual Technical Conference and Exhibition*, Society of Petroleum Engineers, 1998.

[6] S. Wang, R. Mohan, O. Shoham, J. Marrelli, and G. Kouba, "Optimal control strategy and experimental investigation of gas-liquid compact separators," in *SPE Annual Technical Conference and Exhibition*, Society of Petroleum Engineers, 2000.

[7] S. Earni, S. Wang, R. S. Mohan, O. Shoham, and J. D. Marrelli, "Slug detection as a tool for predictive control of glcc© compact separators," *Journal of energy resources technology*, vol. 125, no. 2, pp. 145–153, 2003.

[8] O. Shoham, "Adaptive control technique a solution for glcc© separators," 2003.

[9] M. Leskens, A. Huesman, S. Belfroid, P. Verbeek, A. Fuenmayor, P. Van den Hof, E. Nennie, and R. Henkes, "Fast model based approximation of the closed-loop performance limits of gas/liquid inline separators for accelerated design," *IFAC Proceedings Volumes*, vol. 44, no. 1, pp. 12307–12312, 2011.

[10] T. T. Kristoffersen, C. Holden, S. Skogestad, and O. Egeland, "Control oriented model of gas-liquid cylindrical cyclones," in *Accepted for publication at the American Control Conference (ACC), 2017*, IEEE, 2017.

[11] T. T. Kristoffersen, C. Holden, S. Skogestad, and O. Egeland, "Feedback linearizing control of a gas-liquid cylindrical cyclone," in *Accepted for publication at IFAC World Congress, 2017*, IEEE, 2017.

[12] T. T. Kristoffersen and C. Holden, "Nonlinear model predictive control of a gas-liquid cylindrical cyclone," in *Submitted to the Mediterranean Conference on Control and Automation*, 2017.

[13] N. Hovakimyan and C. Cao, *L1 adaptive control theory: guaranteed robustness with fast adaptation*, vol. 21. Siam, 2010.

[14] H. K. Khalil, *Nonlinear systems*, vol. 3. Prentice hall New Jersey, 2002.

[15] T. I. Fossen and M. J. Paulsen, "Adaptive feedback linearization applied to steering of ships," in *Control Applications, 1992., First IEEE Conference on*, pp. 1088–1093, IEEE, 1992.

[16] P. A. Ioannou and J. Sun, *Robust adaptive control*. Courier Dover Publications, 2012.